

# The GRBs Hubble diagram in quintessential cosmological models

Marek Demianski<sup>1,2,3</sup>, Ester Piedipalumbo<sup>4,5</sup>, Claudio Rubano<sup>4,5</sup>

<sup>1</sup> *Institute for Theoretical Physics, University of Warsaw, Hoza 69, 00-681 Warsaw, Poland*

<sup>2</sup> *Department of Astronomy, Williams College, Williamstown, MA 01267, USA*

<sup>3</sup> *Institute for Interdisciplinary Studies "Artes Liberales", Nowy Swiat 69, 00-046 Warsaw, Poland*

<sup>4</sup> *Dipartimento di Scienze Fisiche, Università di Napoli Federico II, Compl. Univ. Monte S. Angelo, 80126 Naples, Italy*

<sup>5</sup> *I.N.F.N., Sez. di Napoli, Complesso Universitario di Monte Sant' Angelo, Edificio G, via Cinthia, 80126 - Napoli, Italy*

Accepted xxx, Received yyy, in original form zzz

## ABSTRACT

It has been recently empirically established that some of the directly observed parameters of GRBs are correlated with their important intrinsic parameters, like the luminosity or the total radiated energy. These correlations were derived, tested and used to standardize GRBs, i.e., to derive their luminosity or radiated energy from one or more observables, in order to construct an *estimated fiducial* Hubble diagram, assuming that radiation propagates in the standard  $\Lambda$ CDM cosmological model. We extend these analyses by considering more general models of dark energy, and an updated data set of high redshift GRBs. We show that the correlation parameters only weakly depend on the cosmological model. Moreover we apply a local regression technique to estimate, in a model independent way, the distance modulus from the recently updated SNIa sample containing 307 SNIa (Astier et al. 2006), in order to calibrate the GRBs 2D correlations, considering only GRBs with  $z \leq 1.4$ . The derived calibration parameters are used to construct a new GRBs Hubble diagram, which we call the *calibrated* GRBs HD. We also compare the *estimated* and *calibrated* GRBs HDs. It turns out that for the common GRBs they are fully statistically consistent, thus indicating that both of them are not affected by any systematic bias induced by the different standardizing procedures. We finally apply our methods to calibrate 95 long GRBs with the well-known Amati relation and construct the *estimated* and *calibrated* GRBs Hubble diagram that extends to redshifts  $z \sim 8$ . Even in this case there is consistency between these datasets. This means that the high redshift GRBs can be used to test different models of dark energy. We used the *calibrated* GRBs HD to constrain our quintessential cosmological model and derived the likelihood values of  $\Omega_m$  and  $w(0)$ .

**Key words:** Gamma Rays: bursts – Cosmology: distance scale – Cosmology: cosmological parameters

## 1 INTRODUCTION

Recent observations of high redshift supernovae of type Ia (SNIa) revealed that the universe is now expanding at an accelerated rate. This surprising result has been independently confirmed by observations of small scale temperature anisotropies of the cosmic microwave background radiation (CMB) (Astier et al. 2006; Kowalski et al. 2008; Amanullah et al. 2010; Jarosik & al 2010). It is usually assumed that the observed accelerated expansion is caused by a so called dark energy, with unusual properties. The pressure of dark energy  $p_{de}$  is negative and it is related with the positive energy density of dark energy  $\epsilon_{de}$  by  $p_{de} = w\epsilon_{de}$ , where the proportionality coefficient  $w < 0$ . According to the present day estimates, about 75% of matter-energy in the universe is in the form of dark energy, so that now the dark energy is the dominating component in the universe. The nature of dark energy is not known. Proposed so far models of dark energy can be divided, at least, into three groups: a) a non zero cosmological constant, in this case  $w = -1$ , or b) a potential energy of some, not yet discovered, scalar field, or c) effects connected with non homogeneous distribution of matter and averaging procedures. In the last two possibilities, in general,

$w$  is not constant and it depends on the redshift  $z$ . Observations of type Ia supernovae and small scale anisotropies of the cosmic microwave background radiation are consistent with the assumption that the observed accelerated expansion is due to the non zero cosmological constant. However, so far the type Ia supernovae have been observed only at redshifts  $z < 2$ , while in order to test if  $w$  is changing with redshift it is necessary to use more distant objects. New possibilities opened up when it turned out that some of the Gamma Ray Bursts are seen at much higher redshifts, the present record is at  $z = 8.26$  (Greiner et al. 2008). Neither the type Ia supernovae nor the GRBs are true "standard candles". A type Ia supernova is a final stage of evolution of a white dwarf, which is a member of a binary system and accreted enough matter to reach the Chandrasekhar mass limit of  $1.4 M_{\odot}$ . Since the exploding white dwarf always contains mass of about the Chandrasekhar limit, and white dwarfs have similar structure, it is reasonable to assume that when they explode they release approximately the same amount of energy. Sterling Colgate already in 1979 suggested that type Ia supernovae could be used as standard candles (Colgate 1979). When finally, late in nineteen nineties, astronomers were able to observe very distant type Ia supernovae, and used them to determine distances to high redshift galaxies, they discovered that the expansion of the universe, instead of slowing down as expected, is accelerating. Because this conclusion has very important consequences it was prudent to check if type Ia supernovae have the same intrinsic luminosity. It turned out that their intrinsic luminosity varies quite a bit, but with the help of several observational characteristics it can be estimated with an accuracy of about 15%. GRBs are even more enigmatic objects. First of all the mechanism that is responsible for releasing the incredible amounts of energy that typical GRB emits is not yet known (see for instance Meszaros 2006 for a recent review on GRBs). It is also not yet definitely known if the energy is emitted isotropically or is beamed. Despite of these difficulties GRBs are promising objects that can be used to study the expansion rate of the universe at high redshifts (Bradley 2003; Schaefer 2003; Dai et al. 2004; Bloom et al. 2003; Firmani et al. 2005; Schaefer 2007; Li et al. 2008; Amati et al. 2008; Tsutsui et al. 2009). Soon after the BeppoSAX satellite was launched in 1996 an afterglow of now famous GRB970228 has been observed and for the first time it was possible to determine its redshift and conclusively show that GRBs occur at cosmological distances. Since then, new satellites have been launched and it became possible to observationally determine several important parameters of GRBs. First of all, it is now possible to determine not only the light curves but also the spectra of GRB radiation for a wide range of photon energies. Using the observed spectrum it is possible to derive additional parameters, for example the peak photon energy  $E_{peak}$ , at which the burst is the brightest, and the variability parameter  $V$  which measures the smoothness of the light curve (for definitions of these and other parameters mentioned below, see Schaefer (2007)). From observations of the afterglow it is possible to derive another set of parameters, redshift is the most important, and also the jet opening angle  $\Theta_{jet}$ , derived from the achromatic break in the light curve of the afterglow, the time lag  $\tau_{lag}$ , which measures the time offset between high and low energy GRB photons arriving at the detector, and  $\tau_{RT}$  - the shortest time over which the light curve increases by half of the peak flux of the burst. However the most important parameters - the intrinsic luminosity  $L$ , and the total radiated energy  $E_{\gamma}$  are not directly observable. Assuming that GRBs emit radiation isotropically it is possible to relate the peak luminosity,  $L$ , to the observed bolometric peak flux  $P_{bolo}$  by

$$L = 4\pi d_L^2(z, cp) P_{bolo}, \quad (1)$$

where  $d_L$  is the luminosity distance, and  $cp$  denotes the set of cosmological parameters that specify the background cosmological model. Equivalently one can use the total collimation corrected energy  $E_{\gamma}$  defined by

$$E_{\gamma} = 4\pi d_L^2(z, cp) S_{bolo} F_{beam} (1+z)^{-1}, \quad (2)$$

where  $S_{bolo}$  is the bolometric fluence and  $F_{beam} = (1 - \cos \Theta_{jet})$  is the beaming factor. It is clear from these relations that, in order to get the intrinsic luminosity, it is necessary to specify the fiducial cosmological model and its basic parameters. But we want to use the observed properties of GRBs to derive the cosmological parameters. The way out of this complicated circular situation has been proposed by Schaefer (2007) and others, who studied correlations between the directly observed parameters of GRBs ( $E_{peak}$ ,  $\tau_{lag}$ ,  $\Theta_{jet}$ , and  $V$ ) and derived parameters like  $L$  and  $E_{\gamma}$ . In his detailed study of these correlations Schaefer used the standard  $\Lambda$ CDM and a quintessence model in which  $w$  is redshift dependent. He showed that the parameters of correlations between  $L$  or  $E_{\gamma}$  and the observed parameters  $E_{peak}$ ,  $\tau_{lag}$ ,  $\Theta_{jet}$ , and  $V$  only weakly depend on the cosmological model. In conclusion his results show that these correlations can be used to standardize the intrinsic luminosity of GRB bursts and so to transform them into standard candles. Recently Basilikos and Perivolaropoulos (2008) have extended the work of Schaefer, by testing the stability of the correlation parameters with respect to possible evolution with redshift and variations of the basic parameters of the background cosmological model. They concluded that the correlation parameters practically do not depend on the redshift. They assumed that the background cosmological model is the standard  $\Lambda$ CDM model but included the  $\Omega_m$  parameter into the set of fitting parameters. In fact they obtained very similar values of the correlation parameters as those obtained by Schaefer, but the  $\Omega_m$  parameter (even at the  $1\sigma$  level) was poorly determined. Almost at the same time and independently Cardone, Cappozziello and Dainotti (2009) extended the analysis performed by Schaefer, by including more objects and adding one recently discovered correlation between the GRBs X-ray luminosity  $L_X$  and the time  $T_a$ , which is characterizing the late afterglow decay. They then, using a Bayesian procedure, fitted all the correlations, estimating their parameters, considering as a fiducial cosmological model the  $\Lambda$ CDM model, with parameters derived from the WMAP5 data.

Finally to check how their results depend on the parameters of the background cosmological model they fitted the correlations on a parameter grid assuming five different values for  $\Omega_m$  and allowing the dark energy equation of state parameter  $w$  to vary with  $z$  as  $w(z) = w_0 + w_a z/(1+z)$ , where  $(w_0, w_a)$  were restricted to vary in the range  $-1.3 < w_0 < -0.3$  and  $-1 < w_a < 1$ . They have found that the distance modulus defined as

$$\mu(z) = 25 + 5 \log d_L(z, cp), \quad (3)$$

only very weakly depends on the background cosmological model with variations not exceeding 1%. Using a sophisticated statistical procedure and the SNIa data they were able to calibrate the correlation parameters of GRB observables and at the same time to determine basic parameters that specify the background cosmological model (Cardone et al. 2008). The presented so far studies of the correlations between observed parameters of the GRBs used as the background cosmological model either the standard  $\Lambda$ CDM model or a model in which the dark energy equation of state can change by assuming that either  $w(z)$  is a linear function of the redshift or that  $w(z) = w_0 + w_a z/(1+z)$ . Let us note that in recent years a host of very different models of dark energy were proposed, with more complicated dependence of  $w(z)$  and most of them are able to fit at least the SNIa data. It is then very important to investigate how strongly, if at all, the correlation parameters depend on the model of dark energy. In particular it is interesting to ask what happens if  $w(z)$  is rapidly changing in the present epoch and/or when the luminosity distance is noticeably different from the  $\Lambda$ CDM model only at  $z > 2$ . With this aim in mind in this note we present results of our analysis of correlations between the observed parameters of the set of GRBs assembled by Schaefer and later extended by (Cardone et al. 2008) and derived parameters, first by assuming that the background cosmological model is one of the quintessence models and secondly by considering an artificial luminosity distance, which at large redshifts gives much larger distances in comparison with the standard  $\Lambda$ CDM model. To study the first problem we selected one of the quintessence models that we have studied some time ago (Rubano & Scudellaro 2002; Demianski et al. 2005; Pavlov et al. 2002; Rubano et al. 2004), and showed that it is consistent with the basic cosmological tests, like type Ia supernovae, the observed CMB temperature anisotropies power spectrum, and basic parameters of the large scale structure as determined by the 2dFGRS and Sloan Digital Sky surveys. In this model the dark energy is represented by a self interacting scalar field with exponential potential which is minimally coupled to gravity. The parameters of the potential have been chosen in such a way that the coupled Einstein - scalar field dynamical equations describing the flat universe can be analytically integrated, what is clearly of a great advantage in our computations. The energy density of dark energy depends on time and also the dark energy equation of state parameter  $w_\phi$  is time dependent. In Fig. 1 we show how the  $w_\phi$  parameter is changing with the redshift. As is apparent from this figure  $w_\phi$  is rapidly changing for  $0 < z < 5$  and is almost constant and equal to  $-1$  at earlier epochs. We have picked this model precisely because of this dramatic difference between the behaviour of the dark energy in comparison with previously considered background cosmological models. The statistical analysis of the correlation relations between the observed parameters of GRBs and their important intrinsic parameters - the total intrinsic luminosity  $L$  and total emitted energy  $E_\gamma$  performed by Schaefer (2007), Basilikos and Perivolaropoulos (2008) and Cardone et al. (2008) shows that the correlation between  $E_{peak}$  and  $E_\gamma$  seems to be the most robust. The total emitted energy is given by equation (2) and, as it is apparent from this relation, in order to calculate  $E_\gamma$ , it is necessary to specify the background cosmological model. We begin our analysis using the quintessence model with exponential potential with parameters fixed by fitting this model to the set of type Ia supernovae data, the power spectrum of CMB temperature anisotropies and parameters of the observed large scale structure ( for detailed description see Demianski et al. (2005)). Using the luminosity distance derived from this model, we fit our correlations, estimate their parameters, and then we update the *estimated* GRBs Hubble diagram. Then, to check the robustness of the discovered correlations between some of the observed parameters of GRBs and their basic intrinsic properties, we have tested the stability of values of the correlation parameters by considering an ad hoc definition of the luminosity distance that gives much larger distances to objects at  $z > 2$  than either of the models mentioned above. Comparing the likelihood contours in the plane defined by the values of the slope parameter,  $a$ , and the intrinsic scatter,  $\sigma_{int}$ <sup>1</sup>, it turns out that our artificial luminosity distance is changing the maximum likelihood values of the correlation parameters but the difference is not large. However the situation changes when we consider, in the space of parameters, the regions of  $1\sigma$ ,  $2\sigma$  and  $3\sigma$  of confidence for our *crazy* model. It turns out that with respect to the same regions constructed for the quintessential model they overlap only at  $1\sigma$ , but differ consistently at higher levels of confidence.

Moreover we apply a local regression technique to estimate, in a model independent way, the distance modulus from the recently updated SNIa sample containing 307 SNIa, in order to calibrate the GRBs 2D correlations considering only GRBs with  $z \leq 1.4$ . The derived calibration parameters are used to construct a new *calibrated* GRBs Hubble diagram. We also compare the *estimated* and *calibrated* GRBs HDs. We finally apply our methods to calibrate 95 long GRBs with the well-known Amati relation and construct the *estimated* and *calibrated* GRBs Hubble diagram that extends to redshifts  $z \sim 8$ . Even in this case there is consistency between these datasets. This means that the high redshift GRBs can be used to test

<sup>1</sup>  $\sigma_{int}$  is the amount of intrinsic scatter which we expect around the best fit line, due to the *empirical* nature of the studied correlations, as we will clarify in the section 2.

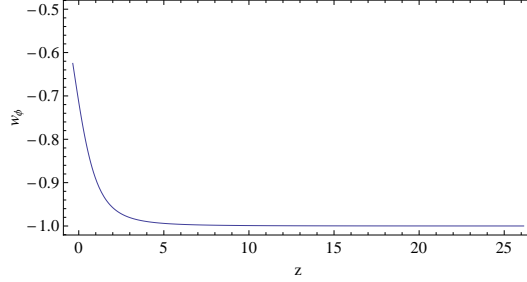


**Figure 1.** The behaviour of the dark energy equation of state parameter  $w_\phi$  on redshift for our fiducial model. It is rapidly changing for  $0 < z < 5$  and is almost constant and equal to  $-1$  at earlier epochs, when the scalar field mimics an effective cosmological constant.

different models of dark energy. We used the *calibrated* GRBs HD to constrain our quintessential cosmological model and to derive the likelihood values of  $\Omega_m$

and  $w(0)$ .

## 2 STANDARDIZING THE GRBS AND CONSTRUCTING THE HUBBLE DIAGRAM

Following (Schaefer 2007; Cardone et al. 2008), we consider six luminosity relations for GRBs. First, we consider five that relate GRB peak luminosity,  $L$ , or the total burst energy in the gamma rays,  $E_\gamma$ , to observables of the light curves and/or spectra:  $\tau_{\text{lag}}$  (time lag),  $V$  (variability),  $E_{\text{peak}}$  (peak of the  $\nu F_\nu$  spectrum), and  $\tau_{\text{RT}}$  (minimum rise time)<sup>2</sup>:

$$\log\left(\frac{L}{1 \text{ erg s}^{-1}}\right) = b_1 + a_1 \log\left[\frac{\tau_{\text{lag}}(1+z)^{-1}}{0.1 \text{ s}}\right], \quad (4)$$

$$\log\left(\frac{L}{1 \text{ erg s}^{-1}}\right) = b_2 + a_2 \log\left[\frac{V(1+z)}{0.02}\right], \quad (5)$$

$$\log\left(\frac{L}{1 \text{ erg s}^{-1}}\right) = b_3 + a_3 \log\left[\frac{E_{\text{peak}}(1+z)}{300 \text{ keV}}\right], \quad (6)$$

$$\log\left(\frac{E_\gamma}{1 \text{ erg}}\right) = b_4 + a_4 \log\left[\frac{E_{\text{peak}}(1+z)}{300 \text{ keV}}\right], \quad (7)$$

$$\log\left(\frac{L}{1 \text{ erg s}^{-1}}\right) = b_5 + a_5 \log\left[\frac{\tau_{\text{RT}}(1+z)^{-1}}{0.1 \text{ s}}\right], \quad (8)$$

where the  $a_i$  and  $b_i$  are fitting parameters. To these known correlations we added a new correlation

$$\log[L_X(T_a)] = b_6 + a_6 \log[T_a/(1+z)], \quad (9)$$

that was recently empirically found by Dainotti et al. (2009) and later confirmed by Ghisellini et al. (2008) and by Yamazaki (2008).

### 2.1 Fitting the correlations and estimating their parameters

In fitting these five calibration relations, we need to fit a data array  $\{x_i, y_i\}$  with uncertainties  $\{\sigma_{x,i}, \sigma_{y,i}\}$ , to a straight line

$$y = b + ax. \quad (10)$$

<sup>2</sup> It is worth noting that the  $E_{\text{peak}} - E_\gamma$  correlation listed below is not physically a 2D correlation, because it involves three observables: the measured fluence, the spectral peak energy and the break time of the optical afterglow light curve needed to measure the jet opening angle. However it can be treated as a 2D correlation from the statistical point of view (to perform the fit).

Eq.(10) is a linear relation which can be fitted to a given data set  $(x_i, y_i)$  in order to determine the two fit parameters  $(a, b)$ <sup>3</sup>. Actually, the situation is not so simple since, both the  $(y, x)$  variables are affected by measurement uncertainties  $(\sigma_x, \sigma_y)$  which can not be neglected. Moreover,  $\sigma_y/y \sim \sigma_x/x$  so that it is impossible to choose as independent variable in the fit the one with the smallest relative error. Finally, the correlations we are fitting are mostly empirical and are not yet derived from an underlying theoretical model determining the detailed features of the GRBs explosion and afterglow phenomenology. Indeed, we do expect a certain amount of intrinsic scatter,  $\sigma_{int}$ , around the best fit line which has to be taken into account and determine together with  $(a, b)$  by the fitting procedure. Different statistical recipes are available to cope with these problems. It is not clear how the fitting technique employed could affect the final estimate of the distance modulus for a given GRB from the different correlations so that it is highly desirable to fit all of them with the same method. Following Cardone et al. (2008), we apply a Bayesian motivated technique (D'Agostini 2005) maximizing the likelihood function  $\mathcal{L}(a, b, \sigma_{int}) = \exp[-L(a, b, \sigma_{int})]$  with:

$$L(a, b, \sigma_{int}) = \frac{1}{2} \sum \ln(\sigma_{int}^2 + \sigma_{y_i}^2 + a^2 \sigma_{x_i}^2) + \frac{1}{2} \sum \frac{(y_i - ax_i - b)^2}{\sigma_{int}^2 + \sigma_{x_i}^2 + a^2 \sigma_{x_i}^2}, \quad (11)$$

where the sum is over the  $\mathcal{N}$  objects in the sample. Note that, actually, this maximization is performed in the two parameter space  $(a, \sigma_{int})$  since  $b$  may be estimated analytically (solving the equation  $\frac{\partial}{\partial b}(L(a, b, \sigma_{int})) = 0$ , as:

$$b = \left[ \sum \frac{y_i - ax_i}{\sigma_{int}^2 + \sigma_{y_i}^2 + a^2 \sigma_{x_i}^2} \right] \left[ \sum \frac{1}{\sigma_{int}^2 + \sigma_{y_i}^2 + a^2 \sigma_{x_i}^2} \right]^{-1}. \quad (12)$$

To quantitatively estimate the goodness of this fit we use the median and root mean square of the best fit residuals, defined as  $\delta = y_{obs} - y_{fit}$  which are computed for the different correlations we consider. To quantify the uncertainties of some fit parameter  $p_i$ , we evaluate the marginalized likelihood  $\mathcal{L}_i(p_i)$  by integrating over the other parameter. The median value for the parameter  $p_i$  is then found by solving:

$$\int_{p_{i,min}}^{p_{i,med}} \mathcal{L}_i(p_i) dp_i = \frac{1}{2} \int_{p_{i,min}}^{p_{i,max}} \mathcal{L}_i(p_i) dp_i. \quad (13)$$

The 68% (95%) confidence range  $(p_{i,l}, p_{i,h})$  are then found by solving (D'Agostini 2005):

$$\int_{p_{i,l}}^{p_{i,med}} \mathcal{L}_i(p_i) dp_i = \frac{1 - \varepsilon}{2} \int_{p_{i,min}}^{p_{i,max}} \mathcal{L}_i(p_i) dp_i, \quad (14)$$

$$\int_{p_{i,med}}^{p_{i,h}} \mathcal{L}_i(p_i) dp_i = \frac{1 - \varepsilon}{2} \int_{p_{i,min}}^{p_{i,max}} \mathcal{L}_i(p_i) dp_i, \quad (15)$$

with  $\varepsilon = 0.68$  and  $\varepsilon = 0.95$  for the 68% and 95% confidence level. Just considering the correlation relation between  $E_\gamma$  and  $E_{peak}$  of the form

$$\log E_\gamma = a \log E_{peak} + b, \quad (16)$$

we find that the likelihood method gives  $a = 1.37$ ,  $b = 50.56$  and  $\sigma_{int} = 0.25$ . In Fig. 2 we show the likelihood contours in the  $(a, \sigma_{int})$  plane and in Fig. 3 we show the correlation between the observed  $\log E_{peak}$  and derived  $\log E_\gamma$  with our assumed background cosmological model. The solid line is the best fit obtained using the D'Agostini's method (D'Agostini 2005) and the dashed line is the best fit obtained by the weighted  $\chi^2$  method. If one marginalizes with respect to  $b$ , then the likelihood values  $a$  and  $\sigma$  are  $a = 1.39$  and  $\sigma = 0.27$ . In Table 1 we present data for the other correlation relations. It is apparent that the correlation parameters only weakly depend on the assumed background cosmological model. Let us stress that in our model the dark energy equation of state is changing and the  $w(z)$  parameter is quite different from the models considered by Schaefer (2007), Basilikos and Perivolaropoulos (2008), and Cardone et al. (2008). To check the robustness of the discovered correlations between some of the observed parameters of GRBs and their basic intrinsic properties we have tested the stability of values of the correlation parameters by considering an ad hoc definition of luminosity distance that places objects with  $z > 2$  at much larger distances than either of the models mentioned above (we call this model a crazy model). First of all in Fig. 4 we show the luminosity distance for our quintessence model (solid line) and the crazy model (dashed line). In this case

<sup>3</sup> For the first five correlations we use the sample of GRBs compiled by Schaefer (2007), while the  $L_X - T_a$  correlation is calibrated using a subsample of the Willingale et al. (2007) catalog made out of 28 GRBs with measured redshift,  $\log L_X(T_a) \geq 45$  and  $1 \leq \log [T_a/(1+z)] \leq 5$  (see (Dainotti et al. 2008) for the motivation of these limits). Moreover we note that  $F_{beam}$  is calculated with the aid of  $d_L(z)$ : for small values of  $\theta_{jet}$ , the dependence of  $F_{beam}$  on  $d_L(z)$  is found to be:  $F_{beam} \propto d_L^{-1/2}$ . Using the data from Schaefer 2007 ( $\Omega_m = 0.27$ ) we have to multiply the corresponding  $F_{beam}$  value by the following factor:  $[d_L^2(0.27, z)/d_L(z, CP)]^{1/2}$

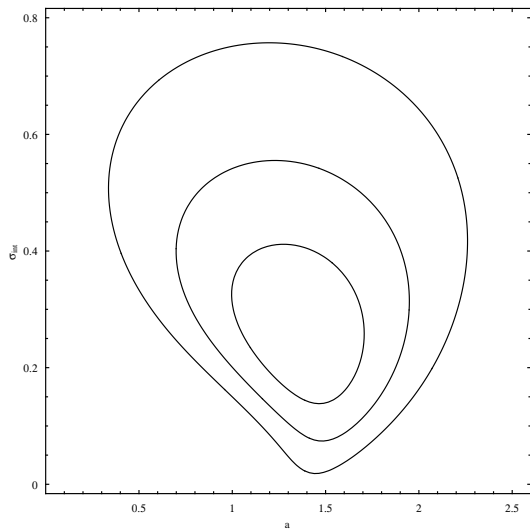


**Figure 2.** Regions of 68%, 95% and 99% of confidence in the space of parameters  $a, \sigma_{int}$ .

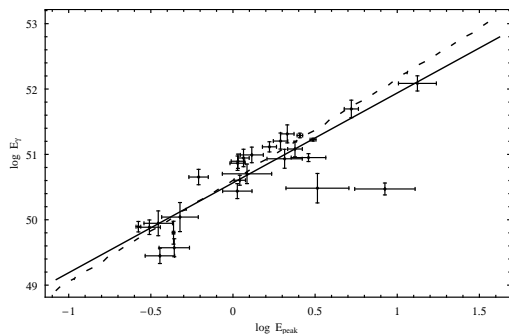


**Figure 3.** Best fit curves for the  $E_{peak} - E_{\gamma}$  correlation superimposed on the data. The solid and dashed lines refer to the results obtained with the Bayesian and Levenberg-Marquardt estimators respectively.

using the likelihood minimalization method we get  $a = 1.69$ ,  $b = 50.60$  and  $\sigma_{int} = 0.30$ . In Fig. 5 we show the 68%, 95% and 99% of confidence in the space of parameters  $a, \sigma_{int}$  for our *crazy* model (red dotted lines), compared with the same regions of confidence for the quintessential model: it is apparent that our artificial luminosity distance is changing the values of the correlation parameters and the regions of confidence. In Fig. 6 we show the correlation between the observed  $\log E_{peak}$  and derived  $\log E_{\gamma}$  with our assumed luminosity distance function. The statistical analysis of the correlation relations between the observed parameters of GRBs and their important intrinsic parameters shows that all the relations have a similar statistical weight since both  $\delta_{med}$  and  $\delta_{rms}$  have almost the same values over the full set, where  $\delta = y_{obs} - y_{fit}$ . This analysis shows only a modest preference for the  $E_{\gamma} - E_p$ ,  $L - \tau_{lag}$  and  $L_X - T_a$  correlations. Taken at face values, the maximum likelihood estimates for  $\sigma_{int}$  favour the  $E_{\gamma} - E_p$  correlation, which seems the most robust, but when one takes into account the 68% and 95% confidence ranges all the correlations overlap quite well. In our analysis we have assumed that the fit parameters do not change with the redshift, which indeed spans a quite large range (from  $z = 0.125$  up to  $z = 6.6$ ). The limited number of GRBs prevents detailed exploration of the validity of this usually adopted working hypothesis, which we tested somewhat investigating if the residuals correlate with the redshift. We have not found any significant correlation. Moreover we tested the fit of the  $E_{\gamma} - E_p$  correlation with respect to the evolution with redshift, separating the GRB samples into four groups corresponding to the following redshift bins:  $z \in [0, 1]$ ,  $z \in [1, 2]$ ,  $z \in [2, 3]$  and  $z \in [3, 7]$ . We thus maximized the likelihood in each group of redshifts and determined the best fit parameters  $a, b$  with  $1\sigma$  errors and the intrinsic dispersion  $\sigma_{int}$ . It turns out that no statistical evidence of a dependence of the  $(a, b, \sigma_{int})$  parameters on the redshift exists. This is in agreement with what has recently been found by Cardone et al. (2008) and Basilakos & Perivolaropoulos (2008).

## 2.2 Constructing the Hubble diagram

Once the six correlations have been fitted, we can now use them to construct the estimated GRBs Hubble diagram. In order to reduce the error and, in a sense, marginalize over the possible systematic biases present in each of the correlations, we take

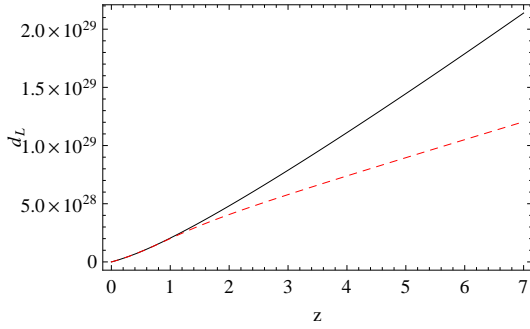


**Figure 4.** The behaviour of the luminosity distance for our quintessence model (solid line) and the crazy model (dashed line).

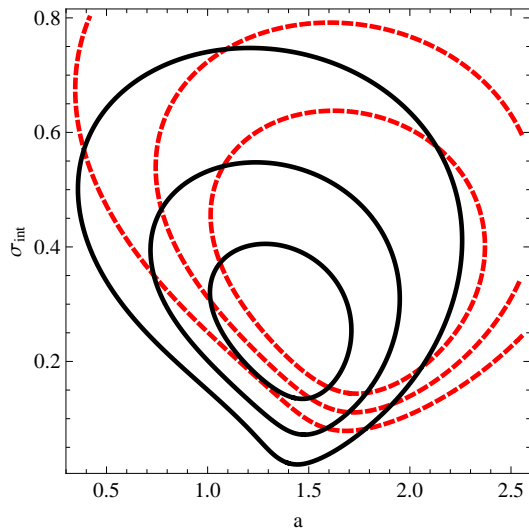


**Figure 5.** Regions of 68%, 95% and 99% of confidence in the space of parameters  $a, \sigma_{int}$  for our *crazy* model (red dashed lines), compared with the same regions of confidence for the quintessential model (solid lines). It turns out that the confidence regions overlap at  $1\sigma$ , but differ consistently at higher levels of confidence.

a weighted average of the distance modulus provided by each of the six 2D laws in Table 1. Just as an example, let us remind that the luminosity distance of a GRB with redshift  $z$  may be computed as :

$$d_L(z) = \begin{cases} E_\gamma(1+z)/4\pi F_{beam} S_{bolo}, \\ L/4\pi P_{bolo}, \\ L_X(1+z)^{\beta_a+2}/4\pi F_X(T_a), \end{cases} \quad (17)$$

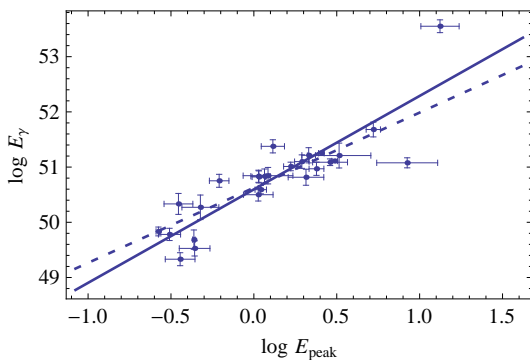


**Figure 6.** Best fit curves for the  $E_{peak} - E_\gamma$  correlation, for our *crazy* model, superimposed on the data. The solid and dashed lines refer to the results obtained with the Bayesian and Levenberg - Marquardt estimators respectively.

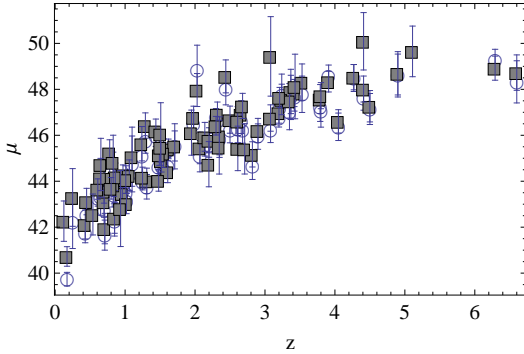


**Figure 7.** The *calibrated* (empty circles) and *estimated* quintessential (full boxes) Hubble diagram.

depending on whether some correlation is used.

The uncertainty of  $d_L(z)$  is then estimated through the propagation of the measurement errors on the involved quantities. In particular, remembering that all the 2D correlation relations can be written as a linear relation, as in Eq. (10), where  $y$  is the distance dependent quantity, while  $x$  is not, the error on the distance dependent quantity  $y$  is estimated as:

$$\sigma(\log y) = \sqrt{a^2 \sigma^2(\log x) + \sigma_{int}^2}, \quad (18)$$

and is then added in quadrature to the uncertainties on the other terms entering Eq.(17) to get the total uncertainty. The distance modulus  $\mu(z)$  is easily obtained from its definition:

$$\mu(z) = 25 + 5 \log d_L(z), \quad (19)$$

with its uncertainty obtained again by error propagation. Following Schaefer (2007) and Cardone et al. (2008), we finally estimate the distance modulus for the  $i$ -th GRB in the sample at redshift  $z_i$  as:

$$\mu(z_i) = \left[ \sum_j \mu_j(z_i) / \sigma_{\mu_j}^2 \right] \times \left[ \sum_j 1 / \sigma_{\mu_j}^2 \right]^{-1}, \quad (20)$$

with the uncertainty given by:

$$\sigma_\mu = \left[ \sum_j 1 / \sigma_{\mu_j}^2 \right]^{-1}, \quad (21)$$

where the sum runs over the considered empirical laws. Joining the Willingale et al. (2007) and Schaefer (2007) samples and considering that 17 objects are in common, we end up with a catalog of 83 GRBs which we use to build the Hubble diagram plotted in Fig. 7. We will refer in the following to this data set as the *fiducial* GRBs Hubble diagram (hereafter, HD) since to compute the distances it relies on the calibration based on the fiducial model. We applied such a procedure first for our quintessence model and then for our artificial *crazy* model. Although the above analysis has shown that the choice of the underlying cosmological model has only a modest impact on the final estimate of the distance modulus, we compared our *estimated fiducial HD* with a model independent calibrated HD, carried out using SNIa as distance indicators. Actually the SNIa Hubble diagram gives the value of  $\mu(z)$  for a subset of the GRBs sample with  $z \leq 1.4$  which can then be used to calibrate the correlations (see (Cardone et al. 2008) for details). Assuming again that this calibration is redshift independent, one can then build up the Hubble diagram at higher redshifts using the calibrated correlations for the remaining GRBs in the sample. We implement here a slightly different version of the local regression approach described in Cardone et al. (2008), modifying some steps in order to improve the computing time (in particular we use a different choice of the weight function and the order of the fitting polynomial-taking). Once we estimated the distance modulus at redshift  $z$  in a model independent way, we can now calibrate the GRBs correlations considering only GRBs with  $z \leq 1.4$  in order to cover the same redshift range spanned by the SNIa data. For such subset of GRBs we apply the Bayesian fitting procedure described above to construct a new GRBs Hubble diagram that we call the *calibrated* GRBs HD. Plotted in Fig. 7, this HD now contains only the 69 Schaefer GRBs since we have not used the  $L_X - T_a$  correlation because it is impossible to calibrate it with the local regression based method. It turns out that the *calibrated* and *estimated* data sets, although containing a different number of objects (83 vs 69), are consistent (see Figs. 7). This qualitative agreement is also confirmed by considering the numbers of GRBs that are more than  $2\sigma$  away from the theoretical fiducial HD.



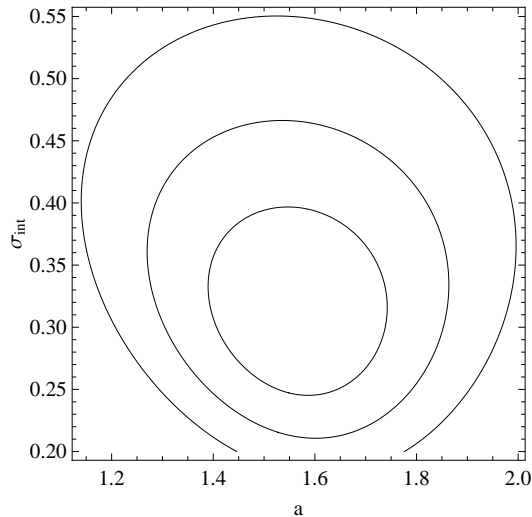


**Figure 8.** Regions of 68%, 95% and 99% of confidence in the space of parameters  $a, \sigma_{int}$ , relatively to the fit of the Amati correlation.

### 3 CONSTRUCTING THE HUBBLE DIAGRAM AND FITTING THE $E_{p,i} - E_{iso}$ CORRELATION

In this section we investigate the possibility of constructing the Hubble diagram from the  $E_{p,i} - E_{iso}$  correlation, here  $E_{p,i}$  is the peak photon energy of the intrinsic spectrum and  $E_{iso}$  the isotropic equivalent radiated energy. This correlation was initially discovered on a small sample of *BeppoSAX* GRBs with known redshifts (Amati et al. 2002) and confirmed afterwards by Swift observations (Amati 2006). Although it was the first correlation discovered for GRBs it was never used for cosmology because of its significant "extrinsic" scatter. However, the recent increase in the efficiency of GRB discoveries combined with the fact that  $E_{p,i} - E_{iso}$  correlation needs only two parameters that are directly inferred from observations (this fact minimizes the effects of systematics and increases the number of GRBs that can be used, by a factor  $\sim 3$ ) makes the use of this correlation an interesting tool for cosmology. Previous analyses of the  $E_{p,i} - E_{iso}$  plane of GRBs showed that different classes of GRBs exhibit different behaviours, and while normal long GRBs and X-Ray Flashes (XRF, i.e. particularly soft bursts) follow the  $E_{p,i} - E_{iso}$  correlation, short GRBs and the peculiar very close and sub-energetic GRBs do not (Amati et al. 2008). This fact depends on the different emission mechanisms involved in the two classes of events and makes the  $E_{p,i} - E_{iso}$  relation a useful tool to distinguish between them (Antonelli 2009). A natural explanation for the short/long dichotomy and the different locations of these classes of events in the  $E_{p,i} - E_{iso}$  plane is provided by the "fireshell" model of GRBs (Ruffini 2009). The impact of selection and instrumental effects on the  $E_{p,i} - E_{iso}$  correlation of long GRBs was investigated since 2005, mainly based on the large sample of BATSE GRBs with unknown redshifts. Different authors came to different conclusions (see for instance (Ghirlanda et al. 2005)). In particular, (Ghirlanda et al. 2005) showed that BATSE events potentially follow the  $E_{p,i} - E_{iso}$  correlation and that the question to clarify is if, and how much, its measured dispersion is biased. There were also claims that a significant fraction of *Swift* GRBs is inconsistent with this correlation (Butler et al. 2007). However, when considering those *Swift* events with peak energy measured by broad-band instruments like, e.g., Konus-WIND or the *Fermi*/GBM or reported by the BAT team in their catalog (Sakamoto et al. 2008) it is found that they are all consistent with the  $E_{p,i} - E_{iso}$  correlation as determined with previous/other instruments (Amati et al. 2009). In addition, it turns out that the slope and normalization of the correlation based on the single data sets provided by GRB detectors with different sensitivities and energy bands are very similar. These facts further support the reliability of the correlation (Amati et al. 2009). In our analysis we considered the sample of 95 long GRB/XRF only, compiled in (Amati et al. 2008) and (Amati et al. 2009). The redshift distribution covers a broad range of  $z$ , from 0.033 to 8.23, thus extending far beyond that of SNIa ( $z < \sim 1.7$ ), and including GRB 092304, the new high- $z$  record holder of Gamma-ray bursts. As above we apply a Bayesian technique (D'Agostini 2005) to fit the  $E_{p,i} - E_{iso}$  correlation, maximizing the likelihood function of Eq. (11). It turns out that our likelihood method gives  $a = 1.56$ ,  $b = 52.77$  and  $\sigma_{int} = 0.31$ . The likelihood contours in the  $(a, \sigma_{int})$  plane are shown in Fig. 8 and finally in Fig. 9 we show the correlation between the observed  $\log E_{peak}$  and derived  $\log E_{iso}$  with our assumed background cosmological model. The solid line is the best fit obtained using the D'Agostini's method (D'Agostini 2005) and the dashed line is the best fit obtained by the weighted  $\chi^2$  method. Marginalizing over  $b$ , the likelihood values for the parameters  $a, \sigma$  are  $a = 1.57$  and  $\sigma = 0.32$  respectively. As in the previous cases we recalibrate also the  $E_{p,i} - E_{iso}$  correlation using the SNIa data. Once such correlations have been calibrated, we can now use them to compute the *estimated* and *calibrated* GRBs Hubble diagram, according to the relations:

$$d_L^2(z) = \frac{E_{iso}(1+z)}{4\pi S_{bolo}}, \quad (22)$$

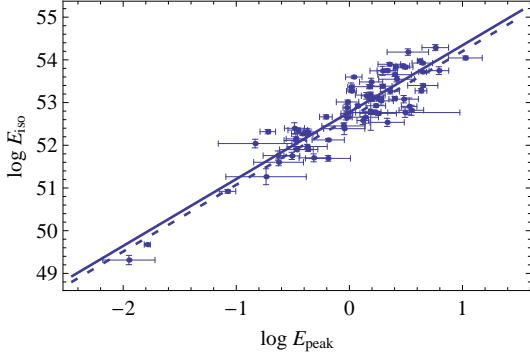


**Figure 9.** Best fit curves, relatively to the fit of the Amati correlation, superimposed on the data: the solid and dashed lines refer to the results obtained with the Bayesian and Levenberg-Marquardt estimators respectively.

$$\mu(z) = 25 + 5 \log d_L(z).$$

It turns out that there are seven GRBs deviating from the fiducial distance modulus  $\mu$  more than  $2\sigma$ ; moreover also for the Amati correlation the *estimated* and *calibrated* HDs are consistent, as shown in Figs. 10 and 11. Moreover, in order to test the reliability of the Amati correlation with respect to the other correlations, we compare the distance modulus  $\mu(z)$  for the *calibrated* Hubble diagram constructed of GRBs dataset used for fitting the five 2D correlations illustrated above and the *calibrated* Hubble diagram constructed of GRBs dataset used for fitting the Amati correlation. However there are only 21 GRBs that appear in both the Schaefer (Schaefer 2007) and Amati (Amati et al. 2009) samples. It turns out that there is full consistency between these datasets (see Fig. 12), and the resulting distances are strongly correlated with the Spearman correlation  $\rho = 0.92$ . We observe that our sample includes 4 GRBs with  $z > 5$ , namely 060522 at  $z = 5.11$ , 050904 at  $z = 6.29$ , 060116 at  $z = 6.60$  and 090423 at  $z = 8.23$ . As is apparent from Fig. 10, there is a clear gap between the  $z > 6$  GRBs and the rest of the sample so that one could wonder whether these objects share the same properties with the other GRBs. Actually, even if extreme in redshift, all of them follow quite well the considered here correlation. In particular the observed properties of 090423 are in a good agreement with the Amati correlation. Therefore, we do not expect that they introduce a bias in the fiducial HD. Moreover, since they are at such a high redshift, they are not used in the calibration based on the local regression analysis. Nevertheless, their distance moduli in the fiducial and calibrated HDs are consistent. We therefore conclude that, notwithstanding the doubts on the validity of this 2D correlation at very high  $z$ , the inclusion of these three GRBs does not bias the results. At the end we use the *calibrated* GRBs Hubble diagram to test if our fiducial cosmological model is able to describe the background expansion up to redshifts  $z \sim 8$ . In the Bayesian approach to model testing, we explore the parameter space through the likelihood function :

$$\mathcal{L}_{GRB}(\mathbf{p}) \propto \exp[-\chi_{GRB}^2(\mathbf{p})/2], \quad (23)$$

with

$$\chi_{GRB}^2(\mathbf{p}) = \sum_{i=1}^{N_{GRB}} \left[ \frac{\mu_{obs}(z_i) - \mu_{th}(z_i)}{\sqrt{\sigma_i^2 + \sigma_{GRB}^2}} \right]^2, \quad (24)$$

where  $\sigma_{GRB}$  takes into account the intrinsic scatter inherited from the scatter of GRBs around the  $E_{p,i} - E_{iso}$  correlation, and  $\mathbf{p}$  denotes the set of model parameters -  $H_0, h$  in our case. The likelihood values are  $H_0 = 0.95 \pm 0.03$   $h = 0.62_{-0.05}^{+0.07}$ , which correspond to  $\Omega_m = 0.26_{-0.04}^{+0.03}$  and  $w(0) = -0.77_{-0.05}^{+0.03}$ . If we marginalize over  $h$  we obtain  $H_0 = 0.93_{-0.03}^{+0.09}$ , which corresponds to  $\Omega_m = 0.31_{-0.09}^{+0.04}$  and  $w(0) = -0.78_{-0.09}^{+0.04}$ .

#### 4 DISCUSSION AND CONCLUSIONS

Recently several interesting correlations among the Gamma Ray Burst (GRB) observables have been identified. Proper evaluation and calibration of these correlations are needed to use the GRBs as standard candles constraining the expansion history of the universe up to redshifts of  $z \sim 8$ . Here we used the GRB data set recently compiled by Schaefer (2007) to investigate, in a quintessential cosmological scenario, the fitting of six 2D correlations: namely  $\tau_{lag}$  (time lag),  $V$  (variability),  $E_{peak}$  (peak of the  $\nu F_\nu$  spectrum), and  $\tau_{RT}$  (minimum rise time). In particular we have investigated the dependence of the calibration, on the assumed cosmological model and a possible evolution of the correlation parameters with the redshift. To check the robustness of the discovered correlations between some of the observed parameters of GRBs and their basic intrinsic properties, we have first tested the stability of values of the correlation parameters by considering an ad hoc definition of luminosity distance that gives much larger distances to objects at  $z > 2$  than either of the fiducial models. It is apparent that

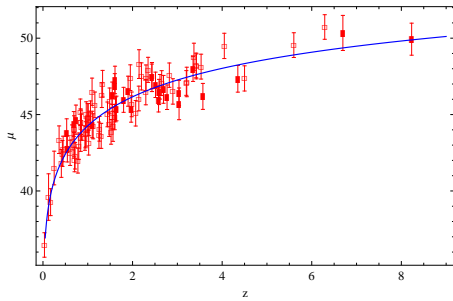


**Figure 10.** The *calibrated* GRBs Hubble diagram with overplotted the distance modulus predicted by the fiducial model. The full boxes correspond to the data set of 70 GRBs compiled by Amati et al. 2008, while the empty ones correspond to the added sample of 20 GRBs compiled by Amati et al. 2009.

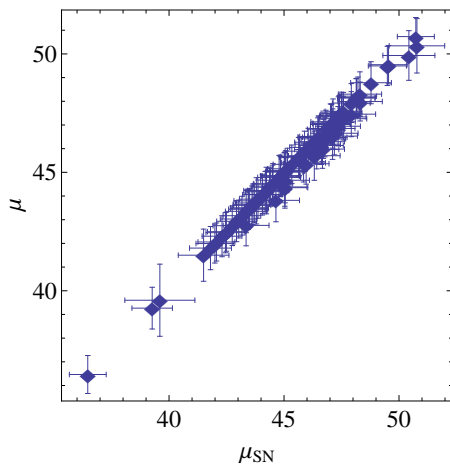


**Figure 11.** Comparison of the distance modulus  $\mu(z)$  for the *calibrated* and *estimated* GRBs Hubble diagram made up fitting the Amati correlation.

our artificial luminosity distance is changing the values of the correlation parameters, however the difference is not dramatic at  $1\sigma$  of confidence, but becomes significant at higher levels. We then investigated the effects of cosmological parameters on the calibration parameters ( $a, b, \sigma_{int}$ ) when we explore the parameters-space of our fiducial cosmological model. It turns out that they very weakly depend on the assumed values of the cosmological parameters. Moreover our analysis shows only a modest preference for the  $E_\gamma - E_p$ ,  $L - \tau_{lag}$  and  $L_X - T_a$  correlations. Taken at face values, the maximum likelihood estimates for  $\sigma_{int}$  favour the  $E_\gamma - E_p$  correlation, which seems the most robust, but when one takes into account the 68% and 95% confidence ranges all the correlations overlap quite well. In our analysis we have assumed that the correlation parameters do not change with the redshift, which indeed spans a quite large range (from  $z = 0.125$  up to  $z = 6.6$ ). The limited number of GRBs prevents detailed exploration of the validity of this usually adopted working hypothesis, which we tested somewhat by investigating if the residuals correlate with the redshift. Moreover we tested the correlation  $E_\gamma - E_p$  with respect to the evolution with redshift, separating the GRB samples into four groups corresponding to the following redshift bins:  $z \in [0, 1]$ ,  $z \in [1, 2]$ ,  $z \in [2, 3]$  and  $z \in [3, 7]$ . We thus maximized the likelihood in each bin of redshift and determined the best fit calibration parameters  $a$ ,  $b$  with  $1\sigma$  errors and the intrinsic dispersion  $\sigma_{int}$ . We have not found any statistical evidence of a dependence of the ( $a, b, \sigma_{int}$ ) parameters on the redshift, as recently also reported by Cardone et al. (2008) and Basilakos & Perivolaropoulos (2008). Once the six correlations have been fitted, we constructed the GRBs Hubble diagram, taking a weighted average of the distance modulus provided by each of the six 2D correlations considered. Although the above analysis has shown that the choice of the underlying cosmological model has only a modest impact on the final estimate of the distance modulus, we apply a local regression technique to estimate, in a model independent way, the distance modulus from the most updated SNIa sample, in order to calibrate the GRBs 2D correlations, including only GRBs with  $z \leq 1.4$ . The derived calibration parameters have been used to construct a new GRBs Hubble diagram, which we call the *calibrated* GRBs HD. We finally compare the *estimated* and *calibrated* GRBs HDs. It turns out that for the common GRBs they are fully statistically consistent thus indicating that both of them are not affected by any systematic bias induced by the different fitting procedures. This means that the high redshift GRBs can be used to test different models of dark energy. We also constructed the Hubble diagram using the  $E_{p,i} - E_{iso}$  correlation, which, recently has been shown to be useful in cosmological considerations. In our analysis we used the sample of 95 long GRB/XRF only, compiled in (Amati et al. 2008) and (Amati et al. 2009), which covers

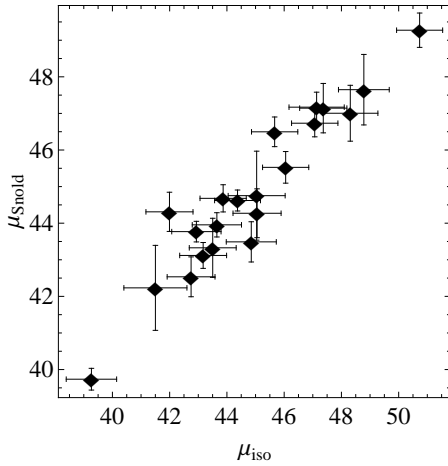


**Figure 12.** Comparison of the distance modulus  $\mu(z)$  for the *calibrated* GRBs Hubble diagram made up by fitting the five  $2 - D$  correlations illustrated above,  $\mu_{Sold}$ , and the *estimated* GRBs Hubble diagram made up by fitting the Amati correlation,  $\mu_{iso}$ , limited to the 21 GRBs that appear in both the Schaefer and Amati samples (Schaefer 2007, Amati et al. 2008, Amati et al. 2009). It turns out that these datasets are fully consistent.

a broad range of  $z$ , and includes GRB 090423, the new high- $z$  record holder of Gamma-ray bursts. As above we calibrated this correlation maximizing our likelihood function. It turns out that our likelihood method gives  $a = 1.56$ ,  $b = 52.77$  and  $\sigma_{int} = 0.31$ . Applying the same Bayesian technique we recalibrate also the  $E_{p,i} - E_{iso}$  correlation using the SNIa data. It turns out that there are seven GRBs deviating from the fiducial distance modulus  $\mu$  more than  $2\sigma$ ; so that also for the Amati correlation the fiducial and calibrated HDs are consistent. We finally use the *calibrated* GRBs Hubble diagram to test if our fiducial quintessential cosmological model is able to describe the background expansion up to redshifts  $z \sim 8$ . The likelihood values correspond to  $\Omega_m = 0.26^{+0.03}_{-0.04}$  and  $w(0) = -0.74^{+0.01}_{0.03}$ . In conclusion one can say that the correlation parameters that relate some of the observed parameters of GRBs with their basic intrinsic parameters only weakly depend on the background cosmological model. This in turn means that the Gamma Ray Bursts could be used to derive values of the basic cosmological parameters and in the future with much larger data set it should be possible to get more information about the nature of dark energy. Since the discovered correlations only weakly depend on the background cosmological model they should be created during the burst itself and therefore they also provide new constrains on models of the Gamma Ray Burst.

## Acknowledgments

This paper was supported in part by the Polish Ministry of Science and Higher Education grant NN202-091839.

## REFERENCES

- Amati L. et al., 2002, A&A, 390, 81  
 Amati L., 2006, MNRAS, 372, 233  
 Amati, L., Guidorzi, C., Frontera, F., et al. 2008, MNRAS, 391, 577  
 Amati, L., Frontera, F., Guidorzi, C., 2009, A&A, 508, 173  
 Amanullah R., &al, 2010, ApJ, 716, 712  
 Antonelli A.L. et al., A&A, 2009, 507, L45  
 Astier, P., Guy, J., Regnault, N., Pain, R., Aubourg, E. et al. 2006, A&A, 447, 31  
 Bradley, S., 2003 ApJ, 583, L67  
 Basilakos, S., Perivolaropoulos, L. 2008, MNRAS, 391, 411  
 Bloom, J.S., Frail, D.A., Kulkarni, S. R., 2003, ApJ, 594, 674  
 Butler N.R. et al., ApJ, 2007, 671, 656  
 Colgate, S. A., 1979, ApJ, 232, 404  
 Cardone, V.F., Capozziello, Dainotti, M.G., S. 2008, MNRAS, 391, L79  
 Dai, Z.G., Liang, E.W., Xu, D. 2004, ApJ, 612, L101  
 Dainotti, M.G., Cardone, V.F., Capozziello, 2009, MNRAS, 400, 775-790  
 Demianski, M., Piedipalumbo, E., Rubano, C., Tortora, C., 2005, A&A, 431, 27  
 Firmani C., Ghisellini, G., Ghirlanda, Avila-Reese, G. 2005, MNRAS, 360, L1  
 Ghirlanda G., Ghisellini G. and Firmani C., 2005, MNRAS, 361, L10.  
 Ghisellini G., Nardini, M., Ghirlanda, G., Celotti, A. 2008, arXiv:0811.1578  
 Greiner, J., Kruehler, T., Fynbo, J.P.U., Rossi, A., Schwarz, R. et al. 2008, arXiv:0810.2314  
 Jarosik N., & al., eprint arXiv:1001.4744

**Table 1.** Calibration parameters ( $a, b$ ), intrinsic scatter  $\sigma_{int}$ , median,  $\delta_{med}$ , and root mean square of the best fit residuals,  $\delta_{rms}$  for the 2D correlations  $\log R = a \log Q + b$  evaluated in two fiducial cosmological models (the  $\Lambda$ CDM and the quintessential exponential scalar field models) and in our crazy model. Columns are as follows: 1. id of the correlation; 2. number of GRBs used; 3. maximum likelihood parameters; 4,5 median value and 68% and 95% confidence ranges for the parameters ( $a, \sigma_{int}$ ); 6,7 median and root mean square of the residuals.

Id	$\mathcal{N}$	$(a, b, \sigma_{int})_{ML}$	$a_{-1\sigma}^{+1\sigma}$	$(\sigma_{int})_{-1\sigma}^{+1\sigma}$	$\delta_{med}$	$\delta_{rms}$
$E_{\gamma}^{\Lambda CDM} - E_p$	27	(1.38, 50.56, 0.25)	$1.37_{-0.26}^{+0.23}$	$0.30_{-0.09}^{+0.11}$	0.01	0.38
$E_{\gamma}^{scalar} - E_p$	27	(1.37, 50.56, 0.25)	$1.37_{-0.26}^{+0.23}$	$0.30_{-0.09}^{+0.16}$	0.01	0.38
$E_{\gamma}^{crazy} - E_p$	27	(1.36, 50.63, 0.25)	$1.69_{-0.26}^{+0.263}$	$0.35_{-0.09}^{+0.12}$	0.01	0.42
$L^{\Lambda CDM} - E_p$	64	(1.24, 52.16, 0.45)	$1.24_{-0.18}^{+0.18}$	$0.48_{-0.07}^{+0.07}$	-0.05	0.51
$L^{scalar} - E_p$	64	(1.40, 51.95, 0.46)	$1.24_{-0.18}^{+0.18}$	$0.48_{-0.07}^{+0.07}$	-0.05	0.51
$L^{crazy} - E_p$	64	(1.57, 52.31, 0.55)	$1.57_{-0.21}^{+0.21}$	$0.58_{-0.08}^{+0.09}$	-0.07	0.52
$L^{\Lambda CDM} - \tau_{lag}$	38	(-0.80, 52.28, 0.37)	$-0.80_{-0.14}^{+0.14}$	$0.40_{-0.07}^{+0.09}$	0.02	0.40
$L^{scalar} - \tau_{lag}$	38	(-1.13, 52.16, 0.32)	$-0.80_{-0.14}^{+0.14}$	$0.40_{-0.07}^{+0.09}$	0.02	0.4
$L^{crazy} - \tau_{lag}$	38	(-0.90, 52.67, 0.50)	$-0.90_{-0.18}^{+0.18}$	$0.54_{-0.09}^{+0.11}$	-0.06	0.68
$L^{\Lambda CDM} - \tau_{RT}$	62	(-0.89, 52.48, 0.44)	$-0.89_{-0.18}^{+0.16}$	$0.46_{-0.06}^{+0.07}$	0.04	0.47
$L^{scalar} - \tau_{RT}$	62	(-0.89, 52.45, 0.44)	$-0.89_{-0.16}^{+0.16}$	$0.46_{-0.06}^{+0.075}$	0.03	0.48
$L^{crazy} - \tau_{RT}$	62	(-1.07, 52.71, 0.63)	$-1.079_{-0.21}^{+0.21}$	$0.66_{-0.08}^{+0.1}$	-0.12	0.69
$L^{\Lambda CDM} - V$	51	(1.03, 52.49, 0.48)	$1.04_{-0.29}^{+0.39}$	$0.51_{-0.07}^{+0.09}$	-0.09	0.50
$L^{scalar} - V$	51	(1.04, 52.47, 0.48)	$1.05_{-0.28}^{+0.29}$	$0.51_{-0.07}^{+0.09}$	-0.09	0.5
$L^{crazy} - V$	51	(1.42, 52.64, 0.59)	$1.41_{-0.35}^{+0.33}$	$0.63_{-0.1}^{+0.12}$	-0.12	0.68
$L_X - T_a$	28	(-0.58, 48.09, 0.33)	$-0.58_{-0.18}^{+0.18}$	$0.39_{-0.11}^{+0.14}$	-0.12	0.43

- Li, H., Su, M., Fan, Z., Dai, Z., Zhang, X. 2008, Phys. Lett. B, 658, 95  
Liang, N., Xiao, W. K., Liu, Y., Zhang, S. N. 2008, ApJ, in press, arXiv:0802.4262  
Kowalski, M., Rubin, D., Aldering, G., Agostinho, R.J, Amadon, A. et al. 2008, arXiv:0804.4142 [astro-ph]  
Meszaros, P., Rep. Prog. Phys., 69, 2259 (2006)  
Rubano, C., Scudellaro, P., 2002, Gen. Rel. Grav., 34, 307  
Pavlov M., Rubano C., Sahzin M.V., Scudellaro P., 2002, Astrophys.J. 566, 619-622  
Rubano C., Scudellaro P., Piedipalumbo E., Capozziello S., Capone M., 2004, Phys.Rev.D, 69, 103510  
Ruffini R., *AIPC Proc.*, 2009, **1111**, 325  
Sakamoto T. et al., ApJ Supp., 2008, 175, 179  
Schaefer, B.E. 2003, ApJ, 583, L67  
Schaefer, B.E. 2007, ApJ, 660, 16  
D'Agostini, G. 2005, arXiv : physics/051182  
Tsutsui, R., Nakamura, T., Yonetoku, D., Murakami T. Tanabe, S., et al. 2009, MNRAS, 394, L31-L35  
Wang, Y., 2008, Phys.Rev.D, 78, 123532  
Wood-Vasey, W.M., Miknaitis, G., Stubbs, C.W., Jha, S., Riess, A.G. et al. 2007, ApJ, 666, 694